Applied Mathematical Modelling 34 (2010) 552–560

Contents lists available at ScienceDirect

Applied Mathematical Modelling

journal homepage: www.elsevier.com/locate/apm

Coarse-grained bifurcation analysis and detection of criticalities of an individual-based epidemiological network model with infection control

Andreas I. Reppas [a], Andreas C. Tsoumanis [b], Constantinos I. Siettos [a,*]

[a] School of Applied Mathematics and Physical Sciences, National Technical University of Athens, GR 157 80, Athens, Greece
[b] School of Chemical Engineering, National Technical University of Athens, GR 157 80, Athens, Greece

ARTICLE INFO

Article history:
Received 10 March 2009
Received in revised form 12 May 2009
Accepted 1 June 2009
Available online 6 June 2009

Keywords:
Multi-scale computations
Bifurcation analysis
Individual-based models
Epidemiology
Control

ABSTRACT

We present and discuss how the so called Equation-free approach for multi-scale computations can be used to systematically study certain aspects of the dynamics of detailed individual-based epidemiological simulators. As our illustrative example, we choose a simple individual-based stochastic epidemic model evolving on a fixed random regular network (RRN). We show how control policies based on the isolation of the infected population can dramatically influence the dynamics of the disease resulting to big-amplitude oscillations. We also address the development of a computational framework that enables detailed epidemiological simulators to converge to their coarse-grained critical points, which mark the onset of the emergent time-dependent solutions as well as to trace branches of coarse-grained unstable equilibria. Using the individual-based simulator we construct the coarse-grained bifurcation diagrams illustrating the dependence of the solutions on the disease characteristics.

1. Introduction

The quest for the efficient modelling, analysis, long-term prediction and control of infectious disease spread is one of the most significant and tough research pursuits of our time.

Towards this aim, various public-health measures and policies have been proposed in order to control the outbreak of diseases in an efficient way. One of the most common strategies is the vaccination of a targeted population [1–3]. Another health measure, which has been frequently used for the control of epidemics, concerns the special treatment (quarantine or isolation) of the infected part of the population [4]. In [5,6] it has been shown that a removal rate – depending on the percentage of the infected people – may result to the eradication of the disease. In [4], the policy of quarantine was used in six different models of infectious diseases. The public intervention of isolation and quarantine has also been used in [7,8] along with clinical data to express the efficiency of those measures in diseases such as SARS, Smallpox, Pandemic Influenza and HIV. In [9] the authors investigate the impact of control measures combining indoor air exchange and air filtration with several public health interventions such as vaccination, isolation, and contact tracing in containing the spread of indoor airborne infections.

The ultimate goal is the design and the development of prevention policies to help control or even extinguish a possible epidemic or even pandemic threat. There is no doubt that mathematical models and systems theory are playing a most valuable role in shedding light on the problem and helping make decisions. A large and intensive research effort is evolving for the development of better and more detailed models teaming up scientists from inter-disciplinary fields ranging from

* Corresponding author. Tel.: +30 210 7723950; fax: +30 210 7721302.
E-mail address: ksiet@mail.ntua.gr (C.I. Siettos).

0307-904X/$ - see front matter © 2009 Elsevier Inc. All rights reserved.
doi:10.1016/j.apm.2009.06.005

molecular biology and epidemiology to sociology and applied mathematics. The studies have proceeded mainly on two fronts. On the one hand, there are the "continuum models" in the form of Ordinary or Partial-integral–differential equations [10–12]. However, due to the complexity of the phenomena, available continuum models are often qualitative caricatures of the reality. On the other hand, there are the so-called object-based models where the system is viewed as a network of interacting discrete entities (individuals, components or objects) [13–17]. These include detailed information of the spreading mechanisms such as the structure of the social network, the mobility and the everyday interactions of each individual, demographics of age, gender and income as well as knowledge in the molecular cell/virus level.

A fundamental prerequisite for the systematically analysis of the dynamics and the design of control processes is the availability of reasonably accurate closed form dynamical models. However, for complex object-based epidemiological models the closures required to formulate continuum models are not usually available. When this is the case, conventional continuum algorithms cannot be used directly for systems level analysis and control-intervention policies design.

In current practice, what is usually done with these detailed individual-scaled epidemiological simulators is simple time-integration: i.e. set-up many initial conditions, for each initial condition create a large enough number of ensemble realizations, probably change some of the rules and then run the detailed dynamics for a long time to investigate how things such as different vaccination policies, malignancy of the virus may influence the spread of an outbreak.

However, this "simple" simulation in time is inadequate for systematic analysis of the emergent coarse-grained dynamics and consequently for control design purposes. For example, important tasks such as the efficient exact location of the critical points that mark the onset of outbreaks and other phenomena such as undesirable big-amplitude epidemic oscillations cannot be easily obtained through just temporal simulations.

In this work, we show how the so-called Equation-free approach [18–22] for multi-scale computations can enable detailed epidemiological simulators to converge to their own open-loop coarse-grained criticalities and trace their open-loop solution branches of unstable equilibria, which cannot be detected by long-run plain temporal simulations. In particular, we address a computational framework under which, (a) one can detect coarse-grained bifurcations such as Neimark–Sacker points that mark the onset of periodic solutions for maps and, (b) trace branches of unstable equilibria. We achieve these tasks by treating the epidemiological simulator as a black-box input–output map of the underlying coarse-grained variables. For illustration purposes, we used an extremely simple individual-based model, which, however, is able to catch a fundamental feature of such problems: the emergence of complex dynamics in the coarse-grained level. We describe the rules governing the evolution of the health-state dynamics and discover, through the proposed approach, how the control policy, that is the way infected individuals are held isolated until they recover, can affect drastically the dynamics of the spreading leading to interesting coarse-grained nonlinear phenomena such as limit cycles, i.e., boom and bust disease outbreaks.

The paper is organized as follows: in Section 2, we present the model within the context of a simplistic social graph. In Section 3, we present the multi-scale computational framework, which can be used to efficiently trace branches of unstable equilibria and detect coarse-grained bifurcations, while in Section 4 we illustrate and discuss the results of our approach; we construct the coarse-grained bifurcation diagrams corresponding to different control policies as well as the one corresponding to the control-free dynamics. We conclude with the main outcomes of our work in Section 5.

2. The model

Here, the epidemic evolves on a regular random graph (RRN) [23,24], which is characterized by a constant connectivity degree d between individuals, here, set equal to four. The graph simulates the social structure of our artificial world involving N individuals. The states of the individuals change over discrete time in a probabilistic manner according to simple rules involving their own states and the states of their links. Each susceptible gets infected with a probability depending on the number of its infected neighbors while the recovery probability varies nonlinearly with the number of the infected neighbors. Infected individuals may be isolated depending on the total number of infected ones in the network.

More specifically, each individual interacts with its links and changes its state, at every discrete time step t, according to the following rules:

Rule #1: An infected individual i infects a susceptible neighbor j with a probability $p_{S\to I}=\lambda$, if an active link exists between them. The probability $p_{S\to I}\in[0,1]$ expresses the infectivity of the disease.

Rule #2: An infected individual withdraws itself with a probability $p_{I\to Q}=\rho$ and gets isolated from its links. Each isolated individual recovers with a probability $p_{Q\to R}=\delta$ at each time step. The transition from the state of infected to the state of isolation at each time step is determined by a function of the number of the overall infected individuals, say $[QI]$, where $[QI]=[I]+[Q]$; $[I],[Q]$ denote the density of the infected and quarantined part of the population, respectively. Actually, this function reflects the infection control policy.

In this work, we used two different types of infection control policies, namely a linear and a sigmoid one given by $p_{I\to Q}=[QI]$ and $p_{I\to Q}=\rho=\frac{1}{1+exp[-15([QI]-0.5)]}$, respectively. A diagram of the above functions is given in Fig. 1.

Rule #3: An infected individual recovers with a probability $p_{I\to R}=\mu$. The probability of recovery depends nonlinearly on the number of infected links at time t, according to the function: $p_{I\to R}=\mu=\frac{y}{1+exp\left[15\left(\frac{n(i)}{d}-0.5\right)\right]}+w$, where $n(i)$ denotes the number of infected links of the infected individual i at time t, $(y+w)$ approximates the recovery probability of an infected individual with no infected links and w approximates the probability that an infected will recover even if all its links are also infected. Fig. 2 depicts $p_{I\to R}$ as a function of the infected links, for $y=0.15$ and $w=0.05$. At this point, we should note that

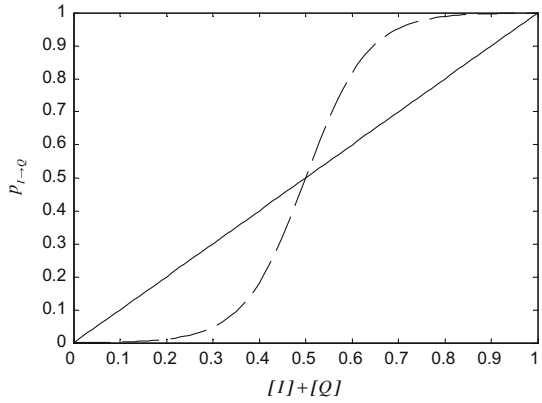

Fig. 1. Probability of an infected to become isolated. These two functions (linear and sigmoid one) determine different control policies of quarantine, i.e. the way an infected individual inactivates its links.

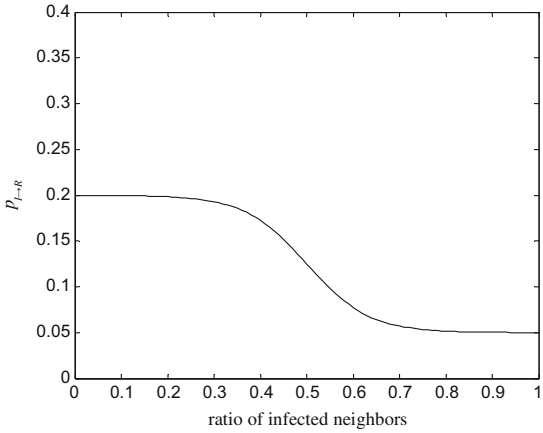

Fig. 2. The function that determines the probability that an infected individual recovers as a function of the infected links for $y = 0.15$, $w = 0.05$.

nonlinear incidence rates have been proposed in the literature to approximate in a better way the emergent dynamics of a disease. For example, the authors in [6,14] use nonlinear incidence rates of the form $k[I]^p[S]^q$ in a system of ordinary differential equations to approximate the emergence and re-emergence of a disease outbreak in a population. Likewise, in [2,7] nonlinear incidence rates were applied in networks of interacting individuals resulting to both stable equilibrium solutions and time-periodic oscillations.

The above relation depicts the fact that when the environment of an infected individual is "contaminated" it makes it more difficult for him to recover and thus his infection persists for a longer time. The nonlinearity may be accounted to different factors such as a drift of the disease-virus over short time periods and heterogeneity in recovery [25].

Rule #4: A recovered individual becomes susceptible with a probability $p_{R\to S} = \varepsilon$. The condition of recovery is a state of temporal immunity: an individual who has suffered in the past acquires immunity for some time until it becomes vulnerable to the disease again.

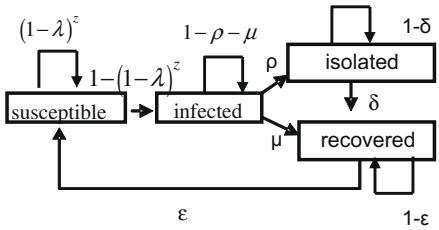

Fig. 3. Flow chart representing the transitions from one state to the others (z = number of infected neighbours with active links).

To this end, Fig. 3 summarizes in a flow chart the rules governing the state transitions in our model.

3. The Equation-free protocol for detecting coarse-grained bifurcations

Our main goal here is to develop a computational framework that can enable detailed individual-based simulators to detect their own coarse-grained bifurcation points. The method uses the Equation-free computational concept and the key assumption of the method is that a coarse-grained model (in the form of ordinary or partial/integral differential equations) for the individual-scale dynamics, in principle exists and closes in terms of (relatively few) coarse-grained variables, but is overwhelming difficult or even impossible to derive [18–22].

The dynamic detailed simulator is only treated as a black box input–output timestepper of the coarse-grained observables. The "black box" coarse timestepper is obtained through the following steps:

(1) Choose the coarse-grained statistics of interest for describing the long-term behavior of the system and an appropriate representation for them (for example the densities of the susceptible and infected individuals in the population).
(2) Choose an appropriate lifting operator $\boldsymbol{\mu}$ from the continuum description $\boldsymbol{u}$ to the individual-based description $\boldsymbol{U}$ on the network. For example, $\boldsymbol{\mu}$ could make random susceptible and infection assignments over the network consistent with the respective densities.
(3) Prescribe a continuum initial condition at a time t_k: $\boldsymbol{u}_{t_k}$.
(4) Transform this initial condition through lifting to one (or more) consistent individual-based realization(s) $\boldsymbol{U}_{t_k} = \boldsymbol{\mu}\boldsymbol{u}_{t_k}$.
(5) Evolve thi(e)s(e) realization(s) using the agent-based model for a desired time T, generating the $\boldsymbol{U}_{t_{k+1}}$, where $t_k = kT$.
(6) *Obtain the restrictions* $\boldsymbol{u}_{t_{k+1}} = \mathbf{M}\boldsymbol{U}_{t_k}$; lifting from the microscopic to the macroscopic and then restricting again should have theoretically no effect, that is, $\mathbf{M}\boldsymbol{\mu} = \mathbf{I}$. *This, constitutes the black-box coarse time-stepper, that, given an initial coarse-grained state of the system* $\boldsymbol{u}_{t_k}$, $\boldsymbol{p}$ *at time* t_k *will report the result of the integration of the individual-based rules after a given time-horizon T (at time* t_{k+1}*), i.e.*

$$\boldsymbol{u}_{t_{k+1}} = \boldsymbol{\Phi}_T(\boldsymbol{u}_{t_k}, \boldsymbol{p}), \tag{1}$$

where $\boldsymbol{\Phi}_T$: $R^n \times R^m \to R^n$ having $\boldsymbol{u}_k$ as initial condition and $\boldsymbol{p}$ denotes the vector of the system parameters.
(7) Augment the fixed-point map equations $\boldsymbol{u} - \boldsymbol{\Phi}_T(\boldsymbol{u}, \boldsymbol{p}) = \mathbf{0}$ by the appropriate condition with regard to the type of criticality sought and wrap around the augmented coarse map a computational superstructural such as simple Newton–Raphson or matrix-free iterative methods (quasi-Newton methods such as the Broyden, Fletcher, Goldfarb, Shanno (BFGS)), direct methods such as the Nelder–Mead algorithm or Newton-GMRES methods [26].

For a fold (or as otherwise called saddle-node) bifurcation and for $m = 1$, the augmented system reads [22]:

$$\begin{bmatrix} \boldsymbol{u} - \boldsymbol{\Phi}_T(\boldsymbol{u}, p) \\ (\boldsymbol{I} - \boldsymbol{J}(\boldsymbol{u}, p))\boldsymbol{q} \\ \|\boldsymbol{q}\| = 1 \end{bmatrix} = \mathbf{0}, \tag{2}$$

where $\boldsymbol{J}(\boldsymbol{u}, p) \equiv \nabla_{\boldsymbol{u}}\boldsymbol{\Phi}_T(\boldsymbol{u}, p)$ is the Jacobian matrix. The second equation in (2) implies that we seek critical points where the Jacobian is singular, a necessary condition for fold bifurcations. Note that in the above formulation the explicit evaluation of the Jacobian is not required. Instead what is needed is the action of the Jacobian $\boldsymbol{J}(\boldsymbol{u}, p)$ on vectors, which can be obtained by calling the coarse black-box timestepper from appropriate nearby initial conditions and for the given time-horizon T.

For a Naimark–Sacker (a nondegenerate, two-dimensional) bifurcation the criticality condition reads [27,28]:

$$\vartheta(\boldsymbol{u}, p) \equiv det[\boldsymbol{J}(\boldsymbol{u}, p)] - 1 = 0. \tag{3}$$

In this case the detection problem can be stated as a constrained minimization problem of the form

$$J = \min_{u \in R^m, p \in R} \left\{ \frac{1}{2}\vartheta(\boldsymbol{u}, p)^2 \right\} \tag{4a}$$

subject to the constraint

$$\boldsymbol{u} - \boldsymbol{\Phi}_T(\boldsymbol{u}, p) = 0. \tag{4b}$$

The same protocol, i.e. steps (1)–(5) can be used for tracing branches of both equilibria and time-dependent solutions. For example the continuation of solution branches past turning points, marking the onset of unstable equilibria (saddles) can be obtained by augmenting Eq. (1) with the linearized pseudo arc-length condition [29]:

$$N(\boldsymbol{u}, p) = \alpha \cdot (\boldsymbol{u} - \boldsymbol{u}_1) + \beta(p - p_1) - \Delta s = 0, \tag{5}$$

where

$$\boldsymbol{\alpha} \equiv \frac{(\boldsymbol{u}_1 - \boldsymbol{u}_0)^T}{\Delta s}, \quad \beta \equiv \frac{(p_1 - p_0)}{\Delta s}$$

and Δs is the pseudo arc-length continuation step. $(\boldsymbol{u}_0, p_0)$ and $(\boldsymbol{u}_1, p_1)$ represent two equilibria that can be found either by temporal simulations or by wrapping around the coarse-timestepper (1) the Newton–Raphson method. The pseudo arc-length condition constrains the consequent solution $(\boldsymbol{u}, p)$ to lie on a hyperplane perpendicular to the tangent of the bifurcation diagram at $(\boldsymbol{u}_1, p_1)$, approximated through $(\boldsymbol{a}, \beta)$ and at a distance Δs from it. The computation of the fixed points can now be obtained using an iterative procedure like the Newton–Raphson technique on the augmented linearized system of (1), (5):

$$\begin{bmatrix} \boldsymbol{I} - \boldsymbol{J} & -\frac{\partial \Phi_T}{\partial p} \\ \boldsymbol{a} & \beta \end{bmatrix} \begin{bmatrix} \delta \boldsymbol{u} \\ \delta p \end{bmatrix} = \begin{bmatrix} \boldsymbol{u} - \boldsymbol{\Phi}_T(\boldsymbol{u}, p) \\ N(\boldsymbol{u}, p) \end{bmatrix}.$$

Note that for the calculation of both the Jacobian $\boldsymbol{J}(\boldsymbol{u}, p)$ and the derivative $\frac{\partial \Phi_T}{\partial p}$, no explicit macroscopic evolution equations are required. They can be approximated numerically by calling the black-box coarse timestepper at appropriately perturbed values of the corresponding unknowns $(\boldsymbol{u}, p)$. Hence, the above framework enables the microscopic simulator to converge to both coarse-grained stable and unstable solutions and trace their locations, i.e. to fulfil tasks that the simulator was not explicitly designed for.

4. Simulation results

For our illustrations, we used the following values for the parameters: $p_{Q\to R} = \frac{1}{3}$, $p_{R\to S} = \frac{1}{3}$, $y = 0.15$, $w = 0.05$. The two different control-policies are compared with the no-control (control-free) action where there is no isolation. We analyzed the coarse-grained behaviour of the epidemic simulator by terms of the parameter $p_{S\to I}$, which served as the bifurcation parameter. For the computations, we used a cluster of 12 nodes running at 2.8 GHz. In all cases, the coarse-grained bifurcation diagrams have been extracted by implementing the Equation-free approach with a time horizon $T = 7$, averaging over 2000 microscopic ensembles.

In the case where there is no isolation, i.e. no control action is deployed, the model is reduced to a Susceptible – Infected – Recovered – Susceptible (SIRS) one with a nonlinear recovery rate. Fig. 4a shows the corresponding coarse-grained bifurcation diagram with respect to $p_{S\to I}$ and Fig. 4b depicts the evolution of the density of the infected population for different values of the infectivity rate. Here the population of infected individuals increases rapidly until it reaches a stationary state for each value of the parameter. As it can be easily seen, the disease is "washed out" for $p_{S\to I} < 0.06$ while dominates in the population above $p_{S\to I} = 0.1$; below this "threshold" the epidemic persists but only a few percentage of the population appears to be infected. However a small increment in $p_{S\to I}$ results to a big increase in the number of infected individuals reaching ~60% of the total population at $p_{S\to I} = 0.2$.

A similar behaviour is observed when applying the linear control policy. The density of infected individuals approaches a stationary state for all the values of the probability $p_{S\to I}$. Fig. 5 shows the corresponding coarse-grained bifurcation diagram depicting the density of the infected part of the population with respect to $p_{S\to I}$. For very small values of the infection probability the only stable solution is the disease-free one. At a critical value around $p_{S\to I} = 0.06$ the disease-free state looses stability through a transcritical bifurcation giving birth to a branch of endemic states, where the susceptible, infected, recovered and quarantined individuals co-exist. Compared to the control-free case for the same values of the parameter $p_{S\to I}$, the linear control policy succeeds to remarkably reduce the percentage of the infected individuals into the population.

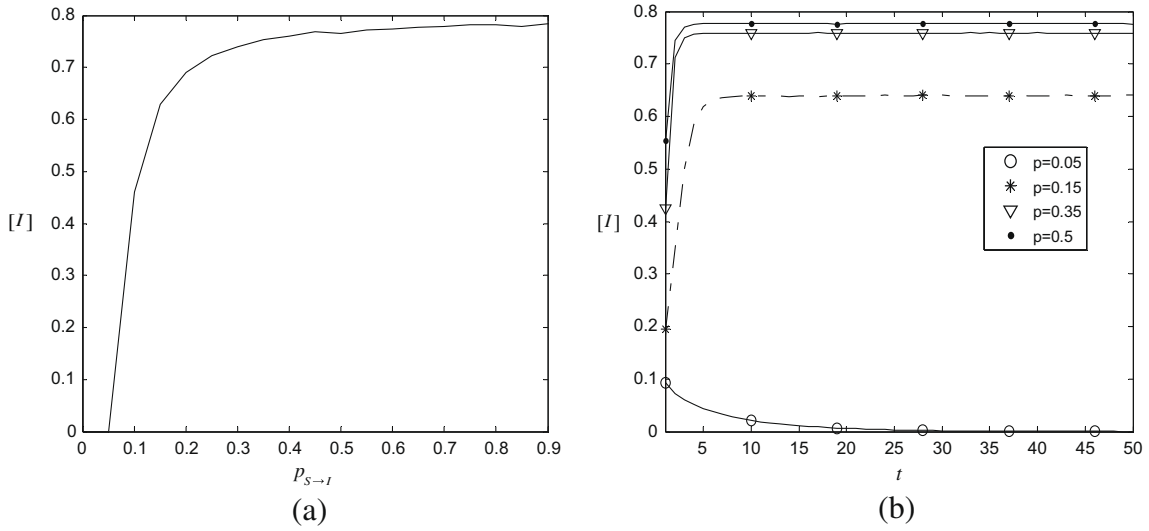

Fig. 4. (a) Coarse-grained bifurcation diagram of the density of infected $[I]$ for the control-free case. (b) Temporal coarse-grained simulations for the control-free case for $p_{S\to I} = 0.05$, 0.15, 0.35 and 0.5.

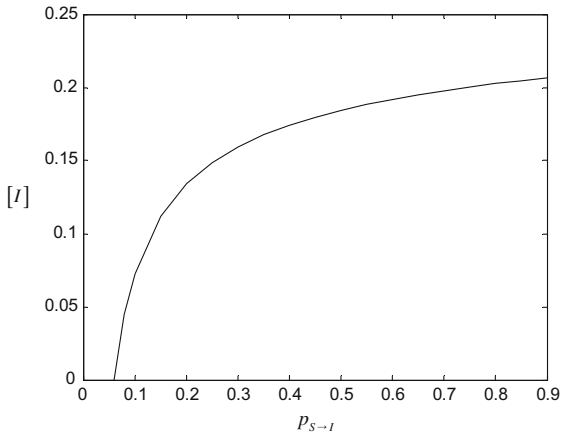

Fig. 5. Coarse-grained bifurcation diagram of the density of the infected individuals $[I]$ with respect to $p_{S\to I}$, linear control policy.

In contrast to the control-free and linear control cases, some interesting nonlinear dynamics emerge when the sigmoid control policy is deployed: depending on the value of $p_{S\to I}$, the system exhibits persistent oscillations leading to periodic boom and bust outbreaks of the infection. For smaller values of the $p_{S\to I}$ the epidemic network follows a similar qualitative behaviour as in the linear control case leading to stationary states (Fig. 6a). However as the $p_{S\to I}$ gets bigger the stationary states loose their stability and the network gives rise to sustained oscillating solutions leading to periodic transitions between high and low infective states (Figs. 6b, and 7). A qualitatively equivalent nonlinear behaviour is observed for a wide range of values of the model parameters.

This behavior indicates the existence of a Neimark–Sacker bifurcation whose exact location was derived using the proposed computational framework. The algorithm used to solve the augmented equations was the Nelder–Mead algorithm [26]. The approach converged to the "correct" coarse-grained bifurcation point at $p^*_{S\to I} \sim 0.51$ as it also approximated by tracing the branch of coarse-grained equilibria past the critical point using the Equation-free approach. Fig. 8 depicts the derived coarse-grained bifurcation diagram. In our difference approximation of the Jacobian, we used perturbations of the order of 10^{-2}. The above computational framework enables the microscopic simulator to converge, to its own coarse-grained stable and unstable (which are not reachable through long run temporal simulations) equilibria and trace their locations with respect to the bifurcation parameter. As it is clearly seen, the sigmoid control policy gives rise to epidemic oscillations of high amplitudes, an undesirable phenomenon which can potentially drive the system to an-all-infected state. The eigenvalues of the Jacobian determine the local stability of the stationary solutions: a coarse-grained fixed point is stable when the norm of all eigenvalues is smaller than one and unstable if there exists at least one eigenvalue with a norm greater than one. Fig. 9 illustrates the pairs of conjugate eigenvalues just before and after the bifurcation point revealing the loss of stability of the coarse-grained fixed point, while Fig. 10 shows the maximum norm of the eigenvalues with respect to the bifurcation parameter around $p^*_{S\to I}$.

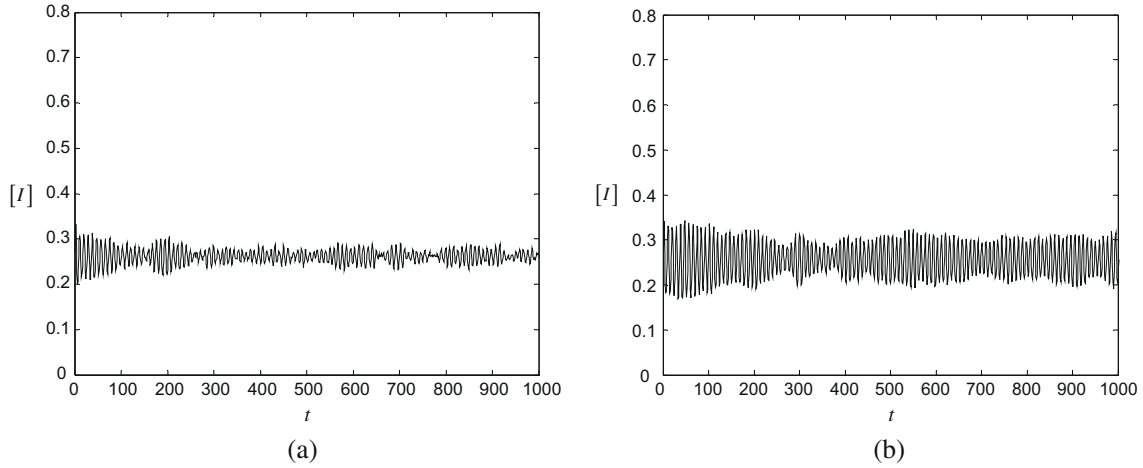

Fig. 6. (a) Time evolution of the density of infected individuals $[I]$ for one copy for $p_{S\to I} = 0.5$ isolation, sigmoid control policy. The system goes to a (noisy) stationary state. (b) Time evolution of the density of infected individuals $[I]$ for $p_{S\to I} = 0.55$, sigmoid control policy. The system oscillates.

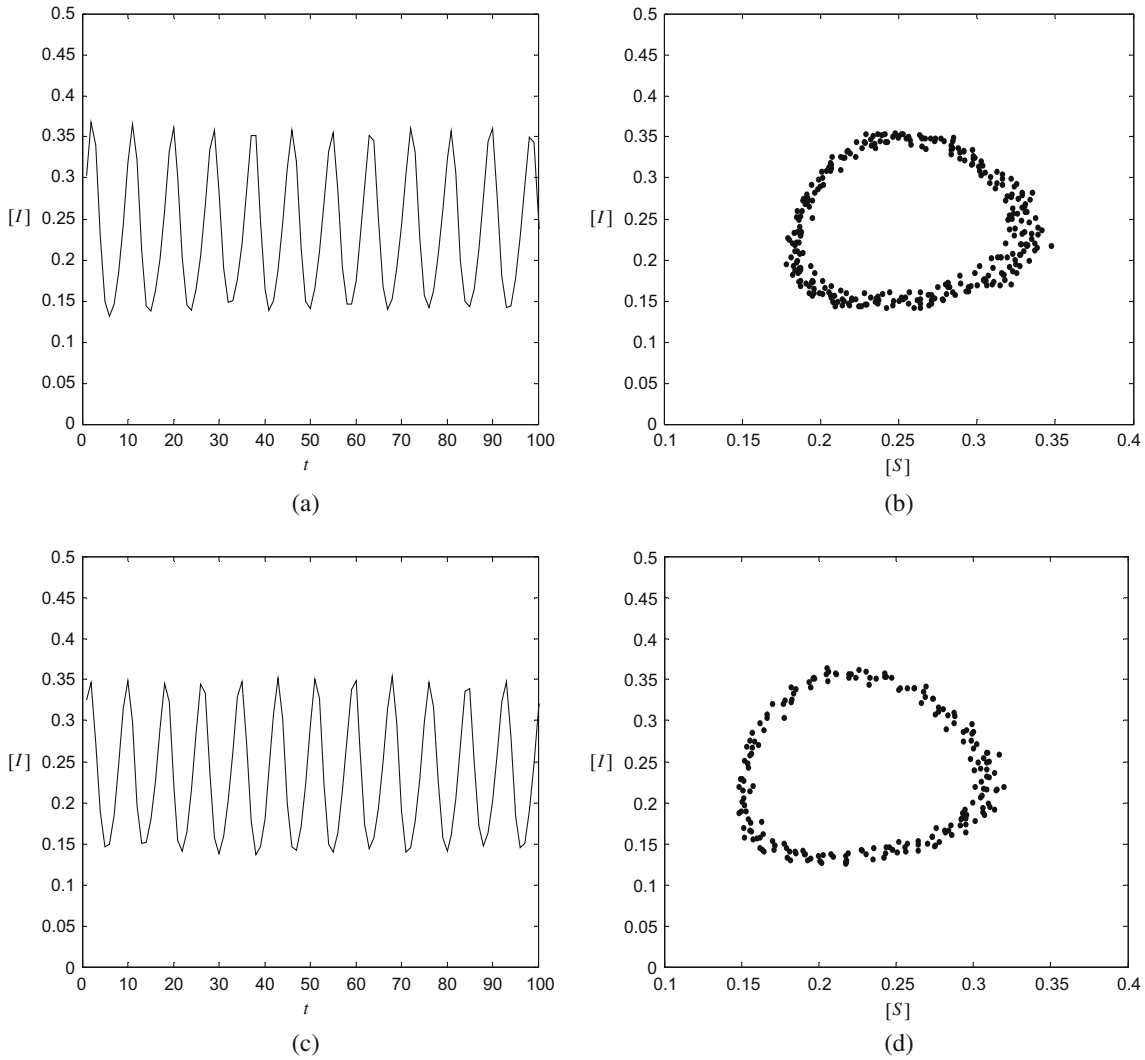

Fig. 7. (a) Time evolution of the density of infected for $p_{S\to I} = 0.7$ using the sigmoid control policy. The system oscillates periodically. (b) Phase diagram of the density of susceptible vs. the density of infected, using the sigmoid control policy when $p_{S\to I} = 0.7$. (c) Time evolution of the density of infected for $p_{S\to I} = 0.9$ using the sigmoid control policy. The solution oscillates. (d) Phase diagram of the density of susceptible over the density of infected, using the sigmoid control policy when $p_{S\to I} = 0.9$.

5. Conclusions

The systematic investigation of the dynamics of fine-scaled epidemic simulators is of outmost importance in practical crisis management and control-intervention design policies. However for such detailed models, the closures required to formulate the problem in the continuum are usually not available and thus traditional numerical analysis and control design algorithms cannot be used. What is currently done with these state-of-the-art simulators is simple temporal simulation. Yet, simulation forward in time is but the first of systems level tasks one wants to explore while analyzing the dynamic behavior of a model. Important tasks such as the efficient exact location of criticalities marking the onset of instabilities and undesirable phenomena such as big-amplitude sustained endemic oscillations cannot be easily obtained through just temporal simulations.

We presented a computational methodology based on the Equation-free framework for multi-scale computations to systematically study certain aspects of the dynamics of individual-based epidemiological simulators. In particular we showed how the framework can be used to effectively detect critical points such as Neimark–Sacker bifurcations and to trace branches of coarse-grained unstable points. This proposed numerically motivated framework may be much more practical and computationally efficient than simple simulation runs. The approach does not rely on the availability of closed form macroscopic equations. It treats the fine-scale simulator as a coarse timestepper to identify "on demand" the quantities that a numerical analysis algorithm would need evaluated from a macroscopic model, had such a model been available, to perform its task.

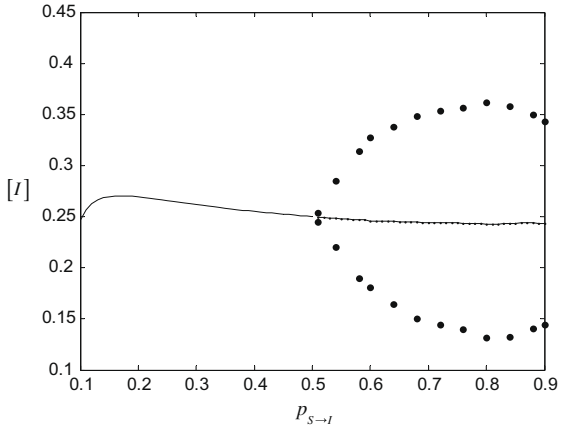

Fig. 8. The coarse-grained bifurcation diagram using the sigmoid control policy. At $p^*_{S\to I} \sim 0.51$ a Neimark–Sacker bifurcation gives birth to a branch of coarse-grained limit cycles. The solid line depicts stable fixed points while dots depict the unstable ones. The circles depict the maximum and the minimum values of the oscillations.

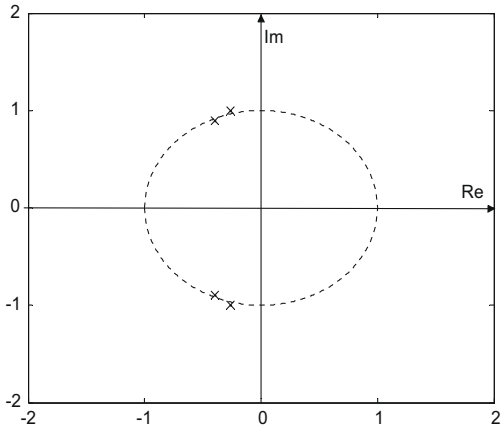

Fig. 9. The pairs of conjugate eigenvalues of the Jacobian matrix estimated at $p_{S\to I} = 0.48$ and $p_{S\to I} = 0.54$. The norm of the eigenvalues when $p_{S\to I} = 0.48$ lies inside the unit circle while when $p_{S\to I} = 0.54$ it is bigger than unity denoting the loss of stability.

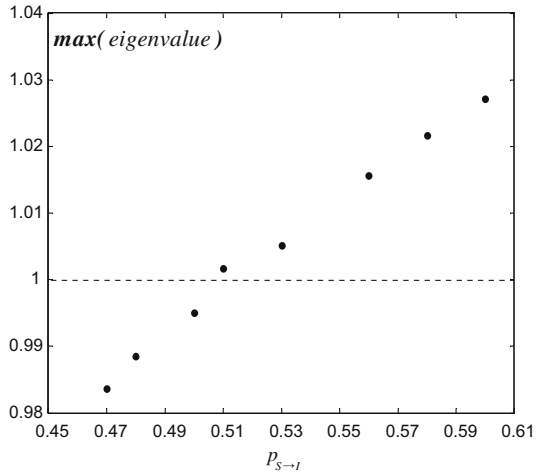

Fig. 10. Maximum norm of the eigenvalues with respect to the bifurcation parameter $p_{S\to I}$. As it is clearly seen, the coarse-grained fixed point loses its stability at the critical value $p^*_{S\to I} \sim 0.51$.

For our illustrations we used an individual-based epidemic model with nonlinear infection-incidence rates incorporating certain disease-spreading control policies. We considered isolation of the infected population as a combat strategy against the transmission of the disease and we evaluated the impacts and the effectiveness of two different control approaches. A comparison of the infection dynamics with the no-control-free case is also illustrated. The proposed model, and depending on the chosen policy, exhibits some interesting nonlinear behavior including sustained periodic oscillations, stable and unstable stationary states.

To get a better understanding of the consequences related with the design of the control-policies we constructed the coarse-grained bifurcation diagrams with respect to the parameter representing the transmission probability of the infection. The analysis revealed that simpler strategies such as a linear dependence between the isolation rate and the percentage of the infected population, meaning action in the early stage of the epidemics, can result in a better control of the spreading. Delayed actions – which may be due to insufficient surveillance and response mechanisms – and vast control efforts at later stages of the epidemics, as this is represented by the sigmoid dependence between the isolation rate and the percentage of the infected population can give rise to undesirable phenomena such as high amplitude persistent oscillations, leading to periodic epidemic outbreaks.

Acknowledgement

This work was partially supported by the National Technical University of Athens through the basic research program "Constantin Caratheodory".

References

[1] M.J. Keeling, The effects of local spatial structure on epidemiological invasions, Proc. Roy. Soc. Lond. 266 (1999) 859–867.
[2] D. Greenhalgh, P. Das, Modelling epidemics with variable contact rates, Theoret. Population Biol. 47 (1995) 129–179.
[3] X. Liu, Y. Takeuchi, S. Iwami, SVIR epidemic models with vaccination strategies, J. Theoret. Biol. 253 (2008) 1–11.
[4] H. Hethcote, Z. Ma, S. Liao, Effects of Quarantine in six endemic models for infectious diseases, Math. Biosci. 180 (2002) 141–160.
[5] S.M. Moghadas, M.E. Alexander, Bifurcation of an epidemic model with non-linear incidence and infection-dependent removal rate, Math. Med. Biol. 23 (2006) 231–254.
[6] W. Wang, S. Ruan, Bifurcations in an epidemic model with constant removal rate of the infectives, J. Math. Anal. Appl. 291 (2004) 775–793.
[7] T. Day, A. Park, N. Madras, A. Gumel, J. Wu, When is quarantine a useful strategy for emerging infectious diseases?, Am J. Epidemiol. 163 (2006) 479–485.
[8] C. Fraser, S. Riley, R.M. Anderson, N.M. Ferguson, Factors that make an infectious disease outbreak controllable, PNAS 101 (2004) 6146–6151.
[9] S.-C. Chen, C.-F. Chang, C.M. Liao, Predictive models of control strategies involved in containing indoor airborn infections, Indoor Air 16 (2006) 469–481.
[10] R.M. Anderson, R.M. May, Population biology of infectious diseases, Nature 280 (1979) 361–367.
[11] F. Brauder, C. Castillo-Chavez, Mathematical Models in Population Biology and Epidemiology, Springer-Verlag, NY, 2001.
[12] J.D. Murray, Mathematical Biology: 1 &2, third ed., Springer, 2007.
[13] N.M. Ferguson, D.A.T. Cummings, S. Cauchemez, C. Fraser, S. Riley, A. Meeyai, S. Iamsirithaworn, D.S. Burke, Strategies for containing an emerging influenza pandemic in Southeast Asia, Nature 437 (2005) 209–214.
[14] I.M. Longini, P.E. Fine, S.B. Thacker, Predicting the global spread of new infectious agents, Am. J. Epidemiol. 123 (1986) 383–391.
[15] S.H. Eubank, V.S.A. Guclu, M. Kumar, M.V. Marathe, A. Srinivasan, Z. Toroczkai, N. Wang, Modelling disease outbreaks in realistic urban social networks, Nature 429 (2004) 180–184.
[16] P.H.T. Schimit, L.H.A. Monteiro, On the basic reproduction number and the topological properties of the contact network: an epidemiological study in mainly locally connected cellular automata, Ecol. Modell. 220 (2009) 1034–1042.
[17] G. Witten, G. Poulter, Simulations of infectious diseases on networks, Comput. Biol. Med. 37 (2007) 195–205.
[18] A. Makeev, D. Maroudas, I.G. Kevrekidis, Coarse stability and bifurcation analysis using stochastic simulators: kinetic Monte Carlo examples, J. Chem. Phys. 116 (2002) 10083–10091.
[19] C.W. Gear, I.G. Kevrekidis, C. Theodoropoulos, Coarse integration/bifurcation analysis via microscopic simulators, Comput. Chem. Eng. 26 (2002) 941–963.
[20] O. Runborg, C. Theodoropoulos, I.G. Kevrekidis, Effective bifurcation analysis: a time-stepper-based approach, Nonlinearity 15 (2002) 491–511.
[21] I.G. Kevrekidis, C.W. Gear, J.M. Hyman, P.G. Kevrekidis, O. Runborg, C. Theodoropoulos, Equation-free coarse-grained multiscale computation: enabling microscopic simulators to perform system-level tasks, Commun. Math. Sci. 1 (4) (2003) 715–762.
[22] C.I. Siettos, R. Rico-Martinez, I.G. Kevrekidis, A systems-based approach to multiscale computation: equation-free detection of coarse-grained bifurcations, Comput. Chem. Eng. 30 (2006) 1632–1642.
[23] B. Bollobás, Random Graphs, second ed., Cambridge University Press, 2001.
[24] M.E.J. Newman, The structure and function of networks, SIAM Rev. 45 (2) (2003) 167–256.
[25] M. Roy, M. Pascual, On representing network heterogeneities in the incidence rate of simple epidemic models, Ecol. Comp. 3 (2006) 80–90.
[26] C.T. Kelley, Iterative Methods for Optimization, SIAM, Philadelphia, 1995.
[27] J.S. Anderson, S.Y. Shvartsman, G. Flätgen, I.G. Kevrekidis, R. Rico-Martinez, K. Krischer, Adaptive method for the experimental detection of instabilities, Phys. Rev. Lett. 82 (1999) 532–535.
[28] Y.A. Kuznetsov, Elements of Applied Bifurcation Theory, second ed., Springer, 1998.
[29] H.B. Keller, Numerical solution of bifurcation and non-linear eigenvalue problems, in: P.H. Rabinowitz (Ed.), Applications of Bifurcation Theory, Academic Press, New York, 1977, pp. 359–384.